

This is a repository copy of *Determining management strategies to control ash dieback disease through the study of molecular and environmental interactions*.

White Rose Research Online URL for this paper:

<https://eprints.whiterose.ac.uk/id/eprint/229377/>

Version: Published Version

Article:

Raykova, Aneliya, Jackson, Joseph, Harper, Andrea Louise orcid.org/0000-0003-3859-1152 et al. (3 more authors) (2025) Determining management strategies to control ash dieback disease through the study of molecular and environmental interactions. *Forests*. 1033. ISSN: 1999-4907

<https://doi.org/10.3390/f16071033>

Reuse

This article is distributed under the terms of the Creative Commons Attribution (CC BY) licence. This licence allows you to distribute, remix, tweak, and build upon the work, even commercially, as long as you credit the authors for the original work. More information and the full terms of the licence here:


<https://creativecommons.org/licenses/>

Takedown

If you consider content in White Rose Research Online to be in breach of UK law, please notify us by emailing eprints@whiterose.ac.uk including the URL of the record and the reason for the withdrawal request.

Article

Determining Management Strategies to Control Ash Dieback Disease Through the Study of Molecular and Environmental Interactions

Aneliya Raykova ^{1,*}, Joseph Jackson ¹, Andrea L. Harper ², Andy Poore ³, Rachael Antwis ¹  and Alexander Mastin ¹

¹ School of Science, Engineering & Environment, University of Salford, Salford M5 4NT, UK; j.a.jackson@salford.ac.uk (J.J.); rachael.antwis@gmail.com (R.A.); alexmastin@gmail.com (A.M.)

² Centre for Novel Agricultural Products (CNAP), Department of Biology, University of York, York YO10 5DD, UK; andrea.harper@york.ac.uk

³ Tollard Royal, Salisbury SP5 5PT, UK; forestry@rushmoreuk.com

* Correspondence: a.raykova@edu.salford.ac.uk

Abstract

Ash dieback (ADB) disease, caused by the devastating fungus *Hymenoscyphus fraxineus* Baral, Queloz & Hosoya, currently poses a significant threat to forest health by decreasing the ash population across the UK and Europe. In our study, we evaluated how environmental conditions, silvicultural management, and genetic factors influence the spread and severity of ash dieback. We combined these factors in a statistical model for susceptibility. Leaves were collected from twenty-two stands across a large semi-natural woodland in Southern England, encompassing a range of disease symptoms. We conducted gene expression assays of tolerance genes previously identified by Associative Transcriptomics and evaluated how stand structure, tree vigour, and individual tree characteristics affected the disease progression. Our results demonstrated that the severity of symptoms is significantly impacted by tree vitality, genetics, and tree size. We identified a diameter at breast height (DBH) group with the highest explained variation (42%) in the disease susceptibility model, with the tree vitality and genetic markers emerging as key determinants. Our findings highlight that lower susceptibility to ash dieback results from a combination of moderate to high genetic tolerance, good individual tree vitality, and appropriate stand management.

Keywords: *Hymenoscyphus fraxineus*; tree vitality; *Fraxinus excelsior*; ADB susceptibility model; Associative Transcriptomics; tree susceptibility



Academic Editors: Young-Seuk Park, Won Il Choi and Jong-Kook Jung

Received: 11 May 2025

Revised: 8 June 2025

Accepted: 9 June 2025

Published: 20 June 2025

Citation: Raykova, A.; Jackson, J.; Harper, A.L.; Poore, A.; Antwis, R.; Mastin, A. Determining Management Strategies to Control Ash Dieback Disease Through the Study of Molecular and Environmental Interactions. *Forests* **2025**, *16*, 1033. <https://doi.org/10.3390/f16071033>

Copyright: © 2025 by the authors. Licensee MDPI, Basel, Switzerland. This article is an open access article distributed under the terms and conditions of the Creative Commons Attribution (CC BY) license (<https://creativecommons.org/licenses/by/4.0/>).

1. Introduction

The invasive fungal pathogen, *Hymenoscyphus fraxineus* Baral, Queloz & Hosoya, the causal agent of ADB disease, poses a critical threat to forest health by decreasing the ash (*Fraxinus excelsior* L.) population across the UK [1] and Europe [2,3]. *Fraxinus excelsior* is native to Great Britain [4], contributing significantly to ecological function [5] and timber production [6], comprising approximately 126 million woodland trees and an additional 27–60 million trees in non-woodland habitats [7]. A small proportion of ash trees have been reported to possess heritable genetic resistance to ADB [8,9]. Reduced susceptibility to *Hymenoscyphus fraxineus* is likely to be a complex trait, including host resistance, disease escape, and tolerance to *H. fraxineus* [10].

Susceptibility to *H. fraxineus* has been shown to have a genetic component [11], and researchers have applied different methods to identify genes associated with low susceptibility [12]. Harper et al. [13] applied Associative Transcriptomics to identify complementary

DNA-based single nucleotide polymorphisms (cDNA-based SNP or cSNPs) and gene expression markers (GEMs) associated with ash dieback damage, offering tools to support future breeding programmes for tolerant trees. In another study, Stocks et al. [14] used a genome-wide association study (GWAS) to identify 3149 SNPs associated with reduced damage caused by *H. fraxineus*. Similarly, research by Meger et al. [15] using a GWAS approach identified six significant SNPs with the potential to enhance genomic selection for future breeding programmes. Susceptibility to ADB varies among individuals of all ages [16,17], outlining smaller trees as very susceptible [18], due to age-related resistance [19]. However, tree size differences might not solely reflect age, but could result from variations in health status and resource competition, as previously reported by Bruce [20]. Ash dieback tends to develop more rapidly and leads to high mortality in small trees [21], while disease progression is slower in mature individuals [16]. Timmermann et al. [21] suggested that higher spore densities and competition between plants close to the forest floor could expedite the disease in juvenile trees, while Lonsdale [22] suggested that fewer symptoms on larger trees could be attributed to the fungus requiring more time to navigate the intricate network of branches and vascular tissues in larger trees but still developing crown dieback [23,24]. The study by Bengtsson et al. [23] also reported that old ash trees growing in shading conditions had greater symptoms of ADB disease. In addition, a study by Madsen et al. [16] reported that old trees had a lower mortality rate, but their health status gradually deteriorated over time and favoured additional biotic stressors, such as *Armillaria* infection, previously found to contribute to the mortality of ash trees [25].

In this context, stand conditions and less vital trees were reported as more susceptible to ADB [26,27]. As reported by Innes [28], tree vitality is a critical factor reflecting forest stand conditions. Dobbartin [29] defined tree vitality as the ability of a tree to grow and maintain its physiological processes under the conditions in which it is growing, therefore reflecting the current stand management, or lack of it. Accumulated stress from pests and pathogens can severely compromise tree vitality [30]. Indeed, field studies in a natural woodland reserve in the UK reported tree vigour as an important determinant of ADB progression [31]. Therefore, maintaining favourable site conditions and implementing suitable forestry practices are crucial for preserving ash trees with lower ADB susceptibility [32]. Silvicultural strategies should prioritise the retention of ash individuals showing tolerance, as non-selective felling would risk the loss of valuable tolerant genotypes [27], with a detrimental impact on forest ecosystems [33]. Thus, retaining ash showing a reasonable level of tolerance would support the general strategies of developing resilient individuals across the forest stand [34].

In this context, we explore the hypothesis that trees with greater vigour before exposure to ADB should be more likely to tolerate and withstand ADB disease, especially if trees are moderately to highly genetically tolerant, not over-mature and subject to other biotic or abiotic problems, nor too small.

Thus, our study aimed to (1) identify environmental and tree-level factors significantly associated with ADB susceptibility; (2) assess the contribution of previously identified genetic markers of tolerance; (3) evaluate the influence of stand conditions on disease progression; and (4) construct a statistical model for disease susceptibility.

2. Materials and Methods

2.1. Experimental Plots

Our study was conducted in 2019–2021. Twenty-two experimental plots were selected from ash-dominated stands at Rushmore Estate (50°56′47.256″ N; 2°6′1.008″ W) (Southern England, Figure S1). The Estate covers a total area of 832.6 ha, of which 430.7 ha (51.7%) contains semi-natural woodland, forming one of the largest surviving blocks of such

woodland in Southern England. The whole Project Area is within a Site of Special Scientific Interest. The forest is also unusual in the level and variety of management, which has produced a particularly high degree of structural and compositional variation across the Project Area.

2.2. Plot-Level Measures

Our twenty-two experimental plots were located within semi-natural broadleaved woodland, and stand structure was classified into seven stand types based on the density of both the canopy and understorey layers, along with the composition of the canopy with regard to the tree size. These structures are associated with different historic management regimes. These plots differ based on their location in the woods, stand type and management systems, understorey characteristics, DBH classes, and density of ash (Tables S1–S3), covering a wide range of ash population structures and site conditions. Within plots, tree age was generally similar across the experimental trees, reflecting typical cohort development.

We also recorded understorey characteristics per plot (Table S3) and collected weather variables (Table S3) from ten experimental plots, 20 May 2019–20 August 2019, comprising 2701 time points for the individual recordings and 68 days for the daily aggregated data. Principal component analysis (PCA) was used to analyse the understorey and weather data.

2.3. Tree-Level Measures

2.3.1. Tree Parameters

Fifteen ash trees were selected in each of the twenty-two plots based on visual observation. The selection criteria included the presence or absence of the fungus, tree and crown sizes of individual ash trees, and their varying level of susceptibility to ADB, ranging from completely healthy to very significantly damaged on different crown sizes to represent the natural diversity of tree conditions, capture the spectrum of host response while maintaining consistency across plots, and avoid bias associated with particular tree health status. Tree replicates (fifteen per plot) were selected along a spiral transect from the centre of the nested area, beginning facing north and continuing to evenly cover the four cardinal directions. In total, 330 trees with different tree sizes and crowns were selected for analysis of crown damage and genetic markers. Individual tree characteristics are listed in Table S2. In our study, we refer to “smaller” trees as individuals within the DBH range of 7–27.99 cm. While DBH was used for categorising trees, we did not use DBH as a proxy for tree vitality. Instead, we used crown cylinder volume (CCV), a volumetric measure of a tree crown size, calculated using two perpendicular crown diameters—D1, the widest horizontal extend of the crown projection area (m), and -D2, the crown diameter measured at a right angle to D1 (m), as a proxy for tree vitality. This approach reflects the rationale that crown size accurately represents the physiological status, competitive conditions, and forest tree vitality [35–37], whereas DBH has been used to integrate cumulative growth and estimates of basal area, tree biomass, and stand growth [38], making it less reflective of recent physiological conditions, such as stress from pathogens. A recent study investigating plant-pathogenic fungal communities also assessed tree vitality based on visual evaluations of crown condition [39]. Three hundred and thirty leaf samples were collected in May 2019 during early morning, aligned with the biology of the timing of *H. fraxineus* ascospore release [40]. Crown dieback assessments were conducted visually in August of 2019, 2020, and 2021 (Table S2) and recorded across seven damage classes (Figure S2).

2.3.2. Quantification of Gene Expression Markers (GEMs)

The protocols for the gene expression markers (GEMs) were conducted as described by Harper et al. [13], except that only GEMs were used for predicting damage scores.

For the quantitative real-time Polymerase Chain Reaction (qRT-PCR) reaction, we used the SYBR[®] Green PCR Master Mix (Applied Biosystems[™], Thermo Fisher Scientific Inc., Waltham, MA, USA), three technical replicates per sample, and a control sample for each gene (forward primer_AshRB_23247: GTCGAGGAGGATGGTCAGTCAT, reverse primer_AshRB_23247_R: AATCTTGCGGAGGACCTATCG; forward primer_AshRB_19216: AGGGCAAGGCTTGGAACAT and reverse primer_AshRB_19216: TAGGCTTTTTTC-TAGCTGCTTGTCAT; Housekeeping gene forward primer_AshRB_GAPDH: CTGGGATCG-CTCTTAGCAAGA and reverse primer_AshRB_GAPDH: CGATCAAATCAATCACAC-GAGAA). The total volume of each RT-PCR reaction was 10 µL, with 3 µL from a 2 ng/µL dilution of cDNA, 5 µL of SYBR Green PCR Master Mix, and 200 nM forward and reverse primers. The RT-PCR thermocycling conditions were as follows: 2 min at 50 °C and 10 min at 95 °C, followed by 40 cycles of 95 °C for 15 s and 60 °C for 1 min, with the final dissociation at 95 °C for 15 s, 60 °C for 1 min, and 95 °C for 15 s. Primer efficiencies were calculated for the target and reference genes (Figures S3–S5). The qRT-PCR data was subsequently analysed using the Pfaffl method (Table S4) [41]. Finally, the gene expression ratios were then used for the subsequent calculations in predicting the ash dieback tolerance algorithm. The GEM prediction values were calculated by standardising and rescaling the Pfaffl–gene expression ratios according to their mean and standard deviation. Finally, the prediction values for each gene were ranked and standardised. The mean of these standardised ranks was then correlated with observed dieback damage scores in the prediction model.

2.3.3. ADB Disease Susceptibility Model

As illustrated in Figure S6, a total of 330 trees and leaf samples were used to conduct the statistical analyses. The data was separated between tree- and plot-level analysis. The tree analysis begins with bivariate statistics (Tables S5 and S6), followed by building the statistical candidate models for generalised linear modelling (GLM) via three approaches to account for the tree age-related confounding effect (DBH used as the stratifier), which is known to influence disease susceptibility and reflect cumulative tree development over time and historic stand conditions: (1st) non-stratified with DBH classes as an interactive term to assess the effect of the interaction term in the model (Table S7); (2nd) non-stratified without the interactive term to assess the significance of the main effect involved in the interaction term (Table S8); (3rd) stratified by DBH approach providing interpretable insights on model variation due to age-related confounding effect under natural setting, where four candidate models were explored in each DBH category (Tables S9–S13). All analyses were conducted using R version 4.1.1 (R Foundation for Statistical Computing, Vienna, Austria) and RStudio version 2024.09.0 + 375 (Posit Software, PBC, Boston, MA, USA) and a model ranking approach; Akaike’s information criterion (AIC) was used to select the best models with MuMIn package, version 1.48.11 (Bartoń, K., accessed via CRAN, R Foundation for Statistical Computing, Vienna, Austria) [42]. Tableau Desktop Professional Edition version 2024.1.1 (Tableau Software LLC, Seattle, WA, USA), and ggplot2 package, version 3.5.2 (Wickham, H., accessed via CRAN, R Foundation for Statistical Computing, Vienna, Austria) [43] were used for data visualisation.

3. Results

3.1. Tree-Level Findings

To assess disease susceptibility at the tree level, we examined the correlations between observed ADB damage and tree-level parameters for all 330 samples. Among the biotic factors, soil pH ($R = -0.22$) and soil temperature ($R = -0.16$) showed weak, but statistically significant negative correlation with damage, suggesting that subtle differences in soil properties may influence host response to infection. Stronger associations were observed

between disease severity and tree parameters. Notably, crown volume ($R = -0.46$) and tree height ($R = -0.43$), were negatively correlated with damage, indicating that larger, more vigorous trees were generally less affected. These results are consistent with previous studies linking tree parameters and reduced disease susceptibility (Havrdova et al. [44]; Erfmeier et al. [24]). Additional crown metrics, including crown height ($R = -0.39$), maximum crown diameter (D1; $R = -0.46$), and its perpendicular diameter (D2; $R = -0.44$), were also exhibiting negative correlations with disease severity based on the full dataset of 330 samples, supporting the hypothesis that increased crown size and leaf area, traits strongly associated with tree vitality, may contribute to disease escape, while recognising the underlying influence of age as a confounding factor. Tree girth and DBH showed similar negative correlations (both ($R = -0.36$)), reinforcing the trend that larger trees were less diseased (Figure S7).

3.1.1. Genetic Tolerance and DBH Stratification

Gene expression markers (GEMs) linked to ADB tolerance, as identified by Harper et al. [13], were scored, standardised, and rescaled into a value between 0 and 100, reflecting the damage score assessment scale. Across all trees, GEMs showed a significant positive correlation with damage scores observed in 2019 ($R = 0.24$), explaining 5.8% of the total variation (Figure S7). While this relationship supports the role of genetic tolerance, stratifying trees by DBH revealed that the associations were not uniform across DBH categories. A strong relationship between GEMs and disease score was observed in DBH categories 1 and 2 (7–27.99 cm and 28–47.99 cm, respectively), with no significant association in larger DBH categories (Figures S8–S10; Tables S14 and S15). Within the DBH categories, the DBH 25–31 cm group demonstrated the strongest explanatory power, where GEMs accounted for 29% of the variation in the observed damage score (Figure S11).

3.1.2. Modelling Tree Susceptibility to ADB

We next developed general linear regression models to quantify the influence of tree characteristics on ADB susceptibility. The models were built on the premise that more vigorous trees (as estimated by crown volume) and those with higher genetic tolerance would be less affected by the disease, containing the following basic parameters: CCV (the proxy to tree vitality); GEMs as an indicator of genetic tolerance; additional tree variables and DBH classes as an interactive terms; and the same ten models, excluding one (Table S8). The optimal model, based on all 330 trees for both, included log-transformed crown cylinder volume (CCV), GEMs, and DBH class as predictors: damage score 2019 ($DS_{2019} \sim \log(CCVC) + GEMs + DBH\ classes$). This model explained 32.8% of the variation in disease scores (adj. $R^2 = 0.3276$; $p < 0.001$), with a low multicollinearity among variables as confirmed by Variance Inflation Factor (VIF) analysis (Table S7).

The direction of effects was consistent with hypotheses that GEMs and DBH class were positively associated with disease tolerance, while CCV was negatively associated with disease severity, indicating that more vigorous and genetically tolerant trees were less susceptible.

3.1.3. Stratified Modelling by Tree Size

To refine the effect of genetics and investigate how disease susceptibility varies across the developmental stages, we constructed four DBH stratified models. For DBH cat. 1 (7–27.99 cm), the best performing model included CCV and GEMs (model c2), explaining 32.5% of the variation (adj. $R^2 = 0.3252$), with GEMs emerging as a significant predictor, whereas DBH recognised as a non-significant predictor contributing to the explanatory power (Table S9). In DBH class 2, the best model also included CCV and GEMs, with CCV showing strong predictive power (adj. $R^2 = 0.25$; Table 1; Table S10). For DBH categories 3

and 4 (larger trees), no significant predictors were identified (Tables S11, S12 and S15), which could indicate that, while genetic factors may still play a role, their influence is potentially less detectable in mature trees compared to earlier developmental stages. However, within the narrower DBH range of 25–31 cm, the combined model incorporating CCV and GEMs explained 42% of the variation in the disease score, which is the highest explanatory power observed in the study (Table 1; Table S13).

Table 1. Summary table demonstrating AIC models, adjusted R^2 , p -values, and AIC values between the explanatory variables and response variable (DS 2019) for different DBH categories.

DBH Cats	AIC Model	Adjusted R^2	AICs Values	Delta	Weight
cat.1 (7–27.99 cm)	DS.2019 ~ log (CCV, 10) *** + log (DBH, 10) + GEMs ***	0.3252	1187.3	0.00	0.448
cat.2 (28–47.99 cm)	DS.2019 ~ log (CCV, 10) *** + GEMs	0.251	1119.2	0.00	0.532
DBH 25–31 cm	DS.2019 ~ log(CCVC, 10) * + GEMs *	0.4239	266.1	0.00	0.770

Significance codes: '***' $p \leq 0.001$, '**' $p \leq 0.05$, $p \leq 0.1$ = not significant.

3.2. Plot-Level Results

3.2.1. Stand Types and Management Practices

Plot-level parameters varied across our experimental plots (Table S16; Figures S12 and S13). While stand types and past management appeared to influence disease severity, no significant relationship was observed between stand density and disease damage (Tables S16 and S17). Our results demonstrated that the Plantation Pole Stage (C, D, L) exhibited the highest average damage score (63%), followed by the Semi-Natural Pole Stage (E, G, F) (56%), with small size DBH consistently showing severe symptoms (Table 2; Figure S14). In contrast, the lower ADB severity was observed at Semi-Natural Irregular Stands (31%). Among management practices, stands that were thinned and fenced in 2003, with understorey cut 2016/2017 exhibited the lowest observed damage (17.83%) (P and Q), which might reflect improved growing conditions, such as reduced competition and herbivore pressure, enhancing physiological function and, in turn, supporting greater tree vitality. Conversely, plots of Plantation origin, particularly C, D, and L, recorded the highest damage (63%) and an average DBH of 15 cm (Figure 1; Table S18). Our analysis of management practices indicates that Irregular High Forest Management is related to lower ADB damage, likely through identifying tolerant trees, implementing appropriate thinning, and removing highly damaged individuals. Collectively, these practices contribute to improved individual tree growing conditions. Although our results show that sites vary in the degree of observed disease severity, we recognise that management may be influenced by factors such as DBH.

Table 2. Stand Type Distribution across the experimental plots at Rushmore Estate and summary data.

Stand Types	Associated Historic Management	Plots	Ave DS. 2019 (%) per Stand Type	Ave DBH per Stand Type	Ave.und/str.comp per Stand Type
Semi-natural Closed	Limited Intervention	S, T, U	36	40	0.499560
Semi-natural Closed + Large Trees.	Limited Intervention	R, I	36	66	1.281481

Table 2. Cont.

Stand Types	Associated Historic Management	Plots	Ave DS. 2019 (%) per Stand Type	Ave DBH per Stand Type	AVE.und/str.comp per Stand Type
Semi-natural Irregular	Irregular High Forest: later development stage	A, B, J, K, P, Q, V	31	40	1.409683
Semi-natural Irregular on Slope	Irregular High Forest: later development stage	N	52	44	0.481481
Semi-natural Transition Pole Stage Dominated	Irregular High Forest: earlier development stage	M, H, W	41	36	0.737654
Semi-natural Pole Stage	Even-aged naturally regenerated 35–40 yrs old	E, G, F	56	14	0.187531
Plantation. Pole Stage	Even-aged plantation: 30–35 yrs old	C, D, L	63	15	0.449250

AVE.und/str.comp: average understorey composition per stand type.

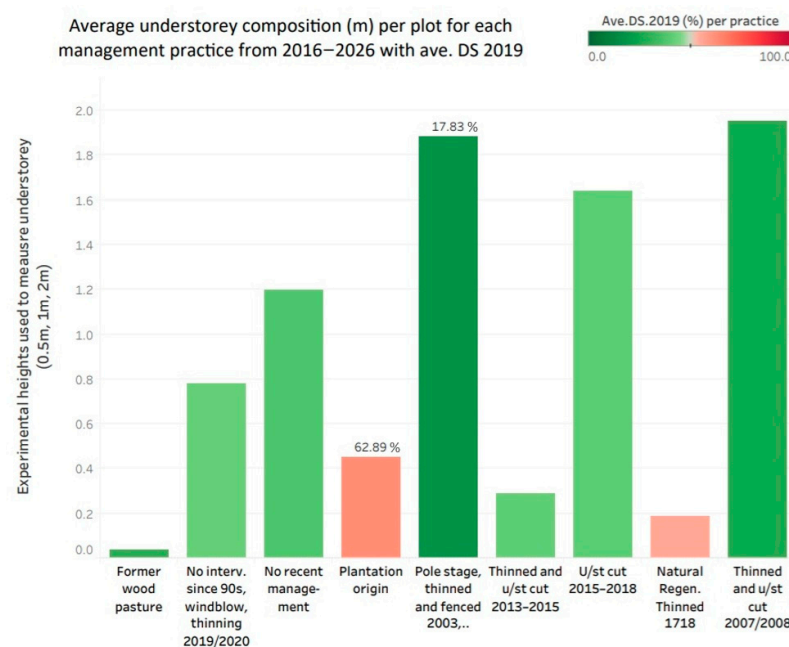


Figure 1. Average understorey composition for each management practice colour-coded with average DS 2019 showing the variation in understorey vegetation measured at three experimental heights (0.5 m, 1.0 m, and 2.0 m), at each cardinal direction in each experimental plot, covering a minimum of 50% of the plot with measurement points per management practices: Former wood pasture; No intervention since 90 s, windblow, Thinning 2019/2020; No recent management; Plantation origin; Pole stage, thinned and fenced in 2003, selection felling, Understorey cut in 2016/2017; Thinned and understorey cut 2013–2015; Understorey cut in 2015–2018; Natural Regenerated P86+, Thinned 1718; Thinned and understorey cut in 2007/2008. The ellipsis (“...”) under the fifth column indicates that pole stage, thinned and fenced in 2003, selection felling, understorey cut in 2016/2017.

3.2.2. Understorey and Weather Analysis

To further explore the ecological context of ADB expression, we performed a principal component analysis (PCA) on the understorey vegetation (Figure S15). The first two components explained 29.2% of the total variation (PC1: 15%; PC2: 14.2%; Figure S15). PC1 was positively associated with high levels of silver birch, dead ivy, hazel, and St John’s wort and negatively with grasses, such as false brome, tufted hair grass, figwort, and thistle (Figures S16 and S17; Table S19). High damage scores were strongly associated

with low PC1 values ($R = -0.71$, $p = 0.0002$; Figure S18; Table S20), suggesting that grass dominated understoreys may coincide with poorer disease outcome, particularly in pole-stage plantation (C, D, E) and naturally regenerated pole-stage plots (F, G) (Figure S17). The PC2 explained 14.2% of the variation and was correlated with high levels of nettle, maple, dead silver birch, hawthorn, and buckthorn and low levels of dead ivy, St John's wort, hazel, and silver birch.

Conversely, plots with low disease damage (e.g., P and Q) were characterised by taller understorey vegetation (>2.5 m) and a dominance of species such as silver birch and hazel. These vegetation assemblages may reflect more favourable microclimatic or competitive conditions. No significant relationships were detected between weather variables and disease damage (Table S21; Figure S19).

4. Discussion

4.1. Factors Affecting Ash Dieback Disease Damage

Our findings support the hypothesis that ADB disease could be influenced by a combination of tree vitality (CCV), genetic tolerance (GEMs), and tree size (DBH), along with site-specific factors such as understorey composition and stand type. Our predictive modelling provides a framework for understanding key parameters influencing ADB susceptibility within its complex dynamics under natural conditions and across different age groups. The strong and significant association between tree vitality (CCV) and ADB severity was in agreement with Cracknell et al. [31], highlighting the importance of tree vitality as a critical factor in modulating disease impact. That said, this association may suggest the possibility of a bidirectional relationship, where tree vitality may assist in compensating for the impact of *H. fraxineus* on ash trees [27,31], possibly reflecting the influence of favourable growing conditions and effective management practices [28]. Conversely, the infection of *H. fraxineus* could potentially contribute to reduced tree vitality by acting as a stressor and facilitating secondary infections [45]. Thus, recognising these interconnected pathways highlights the important role of a robust framework that can effectively support strategies to mitigate the impact of ADB disease.

In field conditions, our gene expression marker (GEM) previously linked to ADB tolerance [13] showed a significant correlation with disease damage across the full dataset of 330 trees, explaining 5.8% of the total variation in disease susceptibility. This relatively low explanatory power likely reflects interactions with tree size, as genetic effects appear to be modulated by the development stage. Similar size-related susceptibility was researched by Klesse et al. [46] and Madsen et al. [16] confirming that tree size and growth dynamics play a significant role in susceptibility to ash dieback progression. Our findings showed that when trees were stratified by DBH categories, the predictive role of GEMs became more apparent. In small trees (DBH 7–27.99 cm), GEMs explained 5.5% of the variation in damage score (Figure S8), increasing to 6.4% in medium trees (DBH 28–47.99 cm; Figure S9). Notably, within the narrower DBH range of 25–31 cm, GEMs explained up to 29% of the variation in the observed damage score (Figure S11), indicating that the influence of genetic tolerance (GEMs) on disease severity may vary across DBH classes, potentially reflecting differences in developmental stage. This aligns with findings by Madsen et al. [16], whose study observed ADB disease progression and mortality in both young and mature ash trees, suggesting that genetic factors influence disease outcomes across age classes. A similar trend was observed with the DBH analysis, where the negative relationship with disease susceptibility outlined that smaller trees were more susceptible than the other DBH classes (Table S7), which is in agreement with a study published by Grosdidier et al. [47] and Klesse et al. [18]. In addition, our analysis showed that all tree parameters significantly correlated with disease susceptibility (Table S5), which is consistent with previous studies

showing an increased susceptibility of trees under stress conditions [27,44], outlining CCV (proxy to tree vitality) as the strongest individual predictor of disease severity ($R = -0.46$). The latter could be explained by the ability of tree vitality to encapsulate both intrinsic resilience and the cumulative effects of environmental stressors and changing conditions and still reproduce [35].

At the plot level, our results indicated the critical roles of stand structure and understorey composition in modulating infection pressure and disease progression. The most severely affected plots were dominated by Semi-Natural and Plantation Pole Stage Stand Types, with an average DBH of just 15 cm (plots C, D, E, F, G, and L). These stands were also associated with dense understorey communities (vegetation height < 0.5 m) and high ash density, both of which are conducive to increased local humidity, greater spore retention, and intensified pathogen spread, factors known to increase infection pressure [27]. Additionally, these conditions have previously been associated with favourable conditions for apothecium development [48] and increased inter-tree competition [49,50], ultimately reducing tree vigour and increasing the mortality rate [18].

In contrast, the least damaged plots (P and Q) were characterised by Semi-Natural Irregular Stand Types, broader DBH sizes including mature trees, and more diverse understorey vegetation dominated by hazel, silver birch, and bracken.

These plots also had lower stand densities of ash, potentially reducing inoculum load and promoting better airflow and light penetration, both of which may inhibit fungal establishment and growth [27]. Collectively, these stand characteristics illustrate that structural heterogeneity and appropriate stand management may enhance stand-level resilience to ADB.

4.2. Ash Dieback Susceptibility Models

4.2.1. Non-Stratified Model

We used linear regression modelling to examine individual tree determinants found to significantly impact the disease progression within one framework. Across all 330 trees, the most informative model included crown cylinder volume (CCV), GEMs, and DBH class, explaining 33% of the total variation in disease damage. VIF scores indicated low collinearity among predictors (Tables S7 and S8) [51]. Some collinearity was expected due to the known positive correlation between DBH and tree crown [52]. This model supports the hypothesis that the combination of trees with large crown volumes (a proxy for tree vitality), that are neither over-mature nor have a small DBH size, combined with favourable genetic profiles, are more likely to be less susceptible to ADB. These findings align with previous research indicating that both physiological conditions and genetic tolerance contribute to mitigating ADB disease, highlighting the importance of integrating multiple tree-level parameters when evaluating risk or selecting management strategies [27,46,53].

4.2.2. Stratified Models by DBH

When trees were stratified by DBH, the most robust model in DBH category 1 explained 33% of the total variation in disease damage, with CCV and GEMs emerging as significant predictors, while DBH itself was non-significant but contributed to the overall predictive power. DBH category 2 and the 25–31 cm subset followed a similar pattern, with models explaining 22% and 42% of the variation, respectively. The enhanced explanatory power in the latter might suggest a developmental stage at which trees are particularly responsive to both genetic and physiological differences. These patterns support the hypothesis that smaller trees, which are in a process of crown development, might be more susceptible to ADB not solely due to their foliage being closer to the forest floor, known to facilitate spore deposition and infection [21], but also due to the compound effect from

site-specific stressors, such as competition and stand management. In such cases, trees might be more reliant on inherent genetic tolerance and vitality to mitigate ADB progression. In contrast, larger or older trees might benefit from structural traits that facilitate faster regeneration and recovery of crown portions [16].

5. Conclusions

Our study demonstrated significant associations between all tree parameters and ADB damage. Furthermore, our GLM model predicted that the combination of trees exhibiting higher vitality (CCV), moderate to high genetic tolerance (GEMs), appropriate age (not too small, or over-mature), and favourable environmental conditions could modulate the impact of ADB severity. Furthermore, the stratified GLM model revealed that in the DBH 25–31 cm category, a robust predictive relationship exists between CCV (proxy for tree vitality) and genetic (GEMs), collectively explaining 42% of the variation in the ADB susceptibility model within this group.

Our results demonstrated the importance of promoting and preserving ash trees that show some genetic tolerance, which will provide a seed source for improved stand tolerance in the future. It should be recognised, however, that trees with very low genetic tolerance, even if they have good vitality and have a benign environment, could succumb to the disease. It is also important to note that while tree vitality can influence ADB severity, the primary cause of the disease is the presence of *H. fraxineus*.

The creation of benign stand conditions can be achieved by the application of silvicultural management strategies aimed at promoting individual tree vitality and maintaining overall stand densities that favour airflow, thus minimising high humidity levels. A key feature of the associated silvicultural practice is selection, both in terms of identifying individuals that have tolerance and favouring them using appropriate thinning, and by the removal of individuals that show higher degrees of damage. Irregular High Forest Management is well suited to delivering these desirable stand characteristics, both in terms of the stand structures produced and the central role of selective harvesting. As a corollary to this, the development of dense pole-stage stands dominated by small ash trees subject to high lateral competition should be avoided.

Supplementary Materials: The following supporting information can be downloaded at <https://www.mdpi.com/article/10.3390/f16071033/s1>, Figure S1: The research study areas at Rushmore Estate, Southern England (A) and twenty-two experimental plots (B); Table S1: Experimental plot characteristics; Figure S2: Visual assessment images of different crown damage percentage; Table S2: Methods used for Trees level measurements [13,41,51,54–56]; Figure S3: Relative contribution and primer efficiency test for the two target genes Gene_19216 and Gene-23247 and the reference GAPDH; Table S3: Methods used for Plot level measurements [57–59]; Figure S4: Amplification plot inspection of the primer efficiency test (Figure S3) using Step One Plus software; Table S4: Pfaffl method; Figure S5: Melt curve inspection for the primer efficiency test (Figure S2) conducted for two target genes: Gene_19216 and Gene-23247 and the reference GAPDH, using Step One Plus software; Table S5: Correlation coefficient (R) calculated between the observed crown damage score (2019) and each tree variables (all 330 samples); Figure S6: Illustration of the analytical approach for the statistical analysis; Table S6: Coefficient of determination (R^2) calculated between the observed crown damage score (2019) and each tree variable (all 330 samples); Figure S7: All diameter classes of *Fraxinus excelsior* damage score percentage (a) and the mean of the two (Gene_19216 and Gene_23247) GEMs genetic markers (b); DBH categories: cat.1 (DBH 7–27.99), cat.2 (DBH 28–47.99), cat.3 (48–67.99), and cat.4 (68–86.99); Table S7: Non-Stratified by DBH susceptibility model with Interactive term (all 330 samples); Figure S8: Small size DBH cat.1 (7–27.99 cm) of *Fraxinus excelsior* damage score percentage (a) and the mean of the two (Gene_19216 and Gene_23247) GEMs genetic markers (b); Table S8: Non-Stratified by DBH susceptibility model with NO Interactive term (all 330 samples); Figure S9:

Medium size DBH cat.2 (28–47.99 cm) of *Fraxinus excelsior* damage score percentage (a) and the mean of the two (Gene_19216 and Gene_23247) GEMs genetic markers (b); Table S9: Stratified by DBH susceptibility model and selection table, DBH cat.1 (7–27.99 cm); Figure S10: Intermediate size DBH cat.3 (48–67.99 cm) (a) and large size DBH cat.4 (68–86.99 cm) (b) of *Fraxinus excelsior* damage score percentage and the mean of the two (Gene_19216 and Gene_23247) GEMs genetic markers; Table S10: Stratified by DBH susceptibility model, DBH cat.2 (28–47.99 cm); Figure S11: DBH 25–31 cm *Fraxinus excelsior* damage score percentage (a) and the mean of the two (Gene_19216 and Gene_23247) GEMs genetic markers (b); Table S11: Stratified by DBH susceptibility model, DBH cat.3 (48–67.99 cm); Figure S12: Boxplot comparison of damage score variation among the twenty-two experimental plots at Rushmore Estate; Table S12: Stratified by DBH susceptibility models, DBH cat.4 (68–86.99 cm); Figure S13: Tree crown average damage score assessments recorded in 2019, 2020, and 2021 (%); Table S13: Stratified by DBH susceptibility models, DBH 25–31 cm; Figure S14: Average understorey composition (m) per plot for each Stand Type Distribution from 2016–2026 with average DS 2019 (colour-coded); Table S14: Stratified approach by DBH to investigate the Coefficient of correlation (R) and Coefficient of determination (R^2 -value) between disease susceptibility and the predictive GEMs marker, along with other tree parameters; Figure S15: Correlation circle of the understorey species measured in 2019 at the experimental plots at Rushmore Estate; Table S15: Summary Table demonstrating AIC models, Adjusted R^2 , p -values, AIC values between the explanatory variables and response variable (DS.2019) for different DBH categories; Figure S16: PCA-biplot representing the grouping of the correlated average understorey species and their associated crown damage score measured in 2019; Table S16: Correlation coefficient (R) calculated between the average of the observed crown damage score (2019) and average plot variables (per plot); Figure S17: Correlations of the average understorey species and PC1 (ordered and coloured by significance); Table S17: Plot Stand Density (Sq/ha); Figure S18: Correlations of the average understorey species and PC2 (ordered and coloured by significance); Table S18: Forest management practices registered at the experimental plots at Rushmore Estate; Figure S19: PCA plot showing the weather variables grouped by plot (ellipse); Table S19: Correlation between the average understorey species and PC1; Table S20: Correlation between the average understorey species and PC2; Table S21: Meteorological variables comparison between the ten experimental plots using Bartlett's test and one-way Anova.

Author Contributions: A.R.: Writing—original draft, Writing—review and editing, Data collection, Fieldwork, Laboratory work, Data analysis, Data visualisation; J.J.: Writing—review and editing, Supervision, Data analysis, A.L.H.: Writing—review and editing, Supervision, Conceptualization, Methodology, Associative Transcriptomics laboratory work and analysis; A.P.: Writing—review and editing, Conceptualization, Methodology, Data analysis; R.A.: Funding acquisition, Conceptualization, Supervision, Writing—review and editing, Data analyses; A.M.: Data analysis, Modelling and multivariate analysis All authors have read and agreed to the published version of the manuscript.

Funding: This research was funded by the University of Salford, Rushmore Estate, Chester Zoo, DEFRA, Natural England, Henry Hoare Charitable Trust, and Salisbury Trust, grant number [ELRC28], and the APC was funded by the University of Salford with funding number [7801085].

Data Availability Statement: Data associated with this study will be made available on request.

Acknowledgments: We are grateful to Andy Taylor and Becky Bevis, who assisted with the fieldwork and accommodation, and Sara Ortega, who helped with the molecular work. We are also grateful to the laboratory technicians from the University of Salford, Marian Denson and Andrew Martin, for their invaluable support and assistance in the laboratory during COVID and the project duration. We also greatly appreciate Ian Goodhead and Stephen Parnell, who supervised and assisted with the PhD project development. We would like to thank the great project collaboration with Sue Walker, Philip Esseen, Emma Goldberg, Joe Alsop, Luise Hill, and Marie Watts for the project administration.

Conflicts of Interest: The authors declare no conflicts of interest.

Abbreviations

The following abbreviations are used in this manuscript:

ADB	Ash dieback (disease)
DBH	Diameter at breast height
GEMs	Gene expression markers
CCV	Crown cylinder volume
PCA	Principal component analysis
AIC	Akaike information criterion
VIF	Variance inflation factor

References

1. Chan, A.H.Y.; Barnes, C.; Swinfield, T.; Coomes, D.A. Monitoring ash dieback (*Hymenoscyphus fraxineus*) in British forests using hyperspectral remote sensing. *Remote Sens. Ecol. Conserv.* **2021**, *7*, 306–320. [\[CrossRef\]](#)
2. McMullan, M.; Rafiqi, M.; Kaithakottil, G.; Clavijo, B.J.; Bilham, L.; Orton, E.; Percival-Alwyn, L.; Ward, B.J.; Edwards, A.; Saunders, D.G.O.; et al. The ash dieback invasion of Europe was founded by two genetically divergent individuals. *Nat. Ecol. Evol.* **2018**, *2*, 1000–1008. [\[CrossRef\]](#) [\[PubMed\]](#)
3. Dobrowolska, D.; Hein, S.; Oosterbaan, A.; Wagner, S.; Clark, J.; Skovsgaard, J.P. A review of European ash (*Fraxinus excelsior* L.): Implications for silviculture. *Forestry* **2011**, *84*, 133–148. [\[CrossRef\]](#)
4. Forestry Commission. Ash Dieback Disease: Pest Alert. 2013. Available online: <https://www.forestryresearch.gov.uk/publications/ash-dieback-disease-pest-alert/> (accessed on 14 April 2019).
5. Mitchell, R.; Beaton, J.; Bellamy, P.; Broome, A.; Chetcuti, J.; Eaton, S.; Ellis, C.J.; Gimona, A.; Harmer, R.; Hester, A. Ash dieback in the UK: A review of the ecological and conservation implications and potential management options. *Biol. Conserv.* **2014**, *175*, 95–109. [\[CrossRef\]](#)
6. FRAXIGEN. *Ash Species in Europe: Biological Characteristics and Practical Guidelines for Sustainable Use*; Oxford Forestry Institute, University of Oxford: Oxford, UK, 2005; 128p.
7. Clark, J.; Webber, J. The ash resource and the response to ash dieback in Great Britain. In *Dieback of European Ash (Fraxinus spp.)—Consequences and Guidelines for Sustainable Management*; Vasaitis, R., Enderle, R., Eds.; Swedish University of Agricultural Sciences: Uppsala, Sweden, 2017; pp. 228–237.
8. Lobo, A.; Hansen, J.K.; McKinney, L.V.; Nielsen, L.R.; Kjær, E.D. Genetic variation in dieback resistance: Growth and survival of *Fraxinus excelsior* under the influence of *Hymenoscyphus pseudoalbidus*. *Scand. J. For. Res.* **2014**, *29*, 519–526. [\[CrossRef\]](#)
9. McKinney, L.V.; Nielsen, L.R.; Hansen, J.K.; Kjær, E.D. Presence of natural genetic resistance in *Fraxinus excelsior* (Oleraceae) to *Chalara fraxinea* (Ascomycota): An emerging infectious disease. *Heredity* **2011**, *106*, 788–797. [\[CrossRef\]](#)
10. Brown, J.; Orton, E. Ashes from Ashes. *Q. J. For.* **2019**, *115*, 107–114.
11. Stocks, J.J.; Buggs, R.J.A.; Lee, S.J. A first assessment of *Fraxinus excelsior* (common ash) susceptibility to *Hymenoscyphus fraxineus* (ash dieback) throughout the British Isles. *Sci. Rep.* **2017**, *7*, 16546. [\[CrossRef\]](#)
12. Downie, J.A. Ash dieback epidemic in Europe: How can molecular technologies help? *PLoS Pathog.* **2017**, *13*, e1006381. [\[CrossRef\]](#)
13. Harper, A.L.; McKinney, L.V.; Nielsen, L.R.; Havlickova, L.; Li, Y.; Trick, M.; Fraser, F.; Wang, L.; Fellgett, A.; Sollars, E.S.A.; et al. Molecular markers for tolerance of European ash (*Fraxinus excelsior*) to dieback disease identified using Associative Transcriptomics. *Sci. Rep.* **2016**, *6*, 19335. [\[CrossRef\]](#)
14. Stocks, J.J.; Metheringham, C.L.; Plumb, W.J.; Lee, S.J.; Kelly, L.J.; Nichols, R.A.; Buggs, R.J.A. Genomic basis of European ash tree resistance to ash dieback fungus. *Nat. Ecol. Evol.* **2019**, *3*, 1686–1696. [\[CrossRef\]](#) [\[PubMed\]](#)
15. Meger, J.; Ulaszewski, B.; Pałucka, M.; Koziol, C.; Burczyk, J. Genomic prediction of resistance to *Hymenoscyphus fraxineus* in common ash (*Fraxinus excelsior* L.) populations. *Evol. Appl.* **2024**, *17*, e13694. [\[CrossRef\]](#) [\[PubMed\]](#)
16. Madsen, C.; Kosawang, C.; Thomsen, I.M.; Hansen, L.N.; Nielsen, L.R.; Kjær, E.D. Combined progress in symptoms caused by *Hymenoscyphus fraxineus* and *Armillaria* species, and corresponding mortality in young and old ash trees. *For. Ecol. Manag.* **2021**, *491*, 119177. [\[CrossRef\]](#)
17. Pastirčáková, K.; Adamčíková, K.; Barta, M.; Pažitný, J.; Hořka, P.; Sarvašová, I.; Kádasi Horáková, M. Host Range of *Hymenoscyphus fraxineus* in Slovak Arboreta. *Forests* **2020**, *11*, 596. [\[CrossRef\]](#)
18. Klesse, S.; Abegg, M.; Hopf, S.E.; Gossner, M.M.; Rigling, A.; Quélou, V. Spread and Severity of Ash Dieback in Switzerland—Tree Characteristics and Landscape Features Explain Varying Mortality Probability. *Front. For. Glob. Change* **2021**, *4*, 645920. [\[CrossRef\]](#)
19. Bruns, E.; Hood, M.; Antonovics, J.; Ballister, I.; Troy, S.; Cho, J.-H. Can disease resistance evolve independently at different ages? Genetic variation in age-dependent resistance to disease in three wild plant species. *J. Ecol.* **2022**, *110*, 2046–2061. [\[CrossRef\]](#)

20. Chadwick, O.; Bruce, L. *Forest Stand Dynamics, Update Edition*; FES Other Publications. 1; Wiley: New York, NY, USA, 1996; Volume 543.
21. Timmermann, V.; Nagy, N.E.; Hietala, A.M.; Børja, I.; Solheim, H. Progression of ash dieback in Norway related to tree age, disease history and regional aspects. *Baltic. For.* **2017**, *23*, 150–158.
22. Lonsdale. *Ancient and Other Veteran Trees: Further Guidance on Management*; The Tree Council: London, UK, 2013.
23. Bengtsson, V.; Stenström, A.; Wheeler, C.P.; Sandberg, K. The impact of ash dieback on veteran trees in southwestern Sweden. *Balt. For.* **2021**, *27*, 2–9. [\[CrossRef\]](#)
24. Erfmeier, A.; Haldan, K.L.; Beckmann, L.-M.; Behrens, M.; Rotert, J.; Schrautzer, J. Ash Dieback and Its Impact in Near-Natural Forest Remnants—A Plant Community-Based Inventory. *Front. Plant Sci.* **2019**, *10*, 658. [\[CrossRef\]](#)
25. Chandelier, A.; Gerarts, F.; San Martin, G.; Herman, M.; Delahaye, L. Temporal evolution of collar lesions associated with ash dieback and the occurrence of *Armillaria* in Belgian forests. *For. Pathol.* **2016**, *46*, 289–297. [\[CrossRef\]](#)
26. Skovsgaard, J.P.; Thomsen, I.M.; Skovsgaard, I.M.; Martinussen, T. Associations among symptoms of dieback in even-aged stands of ash (*Fraxinus excelsior* L.). *For. Pathol.* **2010**, *40*, 7–18. [\[CrossRef\]](#)
27. Skovsgaard, J.P.; Wilhelm, G.J.; Thomsen, I.M.; Metzler, B.; Kirisits, T.; Havrdová, L.; Enderle, R.; Dobrowolska, D.; Cleary, M.; Clark, J. Silvicultural strategies for *Fraxinus excelsior* in response to dieback caused by *Hymenoscyphus fraxineus*. *For. Int. J. For. Res.* **2017**, *90*, 455–472. [\[CrossRef\]](#)
28. Innes, J.L. *Forest Health: Its Assessment and Status*; CAB International: Wallingford, UK, 1993; 677p.
29. Dobbertin, M. Tree growth as indicator of tree vitality and of tree reaction to environmental stress: A review. *Eur. J. For. Res.* **2005**, *124*, 319–333. [\[CrossRef\]](#)
30. Paap, T.; Burgess, T.I.; Wingfield, M.J. Urban trees: Bridge-heads for forest pest invasions and sentinels for early detection. *Biol. Invasions* **2017**, *19*, 3515–3526. [\[CrossRef\]](#)
31. Cracknell, D.J.; Peterken, G.F.; Pommerening, A.; Lawrence, P.J.; Healey, J.R. Neighbours matter and the weak succumb: Ash dieback infection is more severe in ash trees with fewer conspecific neighbours and lower prior growth rate. *J. Ecol.* **2023**, *111*, 2118–2133. [\[CrossRef\]](#)
32. Fuchs, S.; Häuser, H.; Peters, S.; Knauf, L.; Rentschler, F.; Kahlenberg, G.; Kätzel, R.; Evers, J.; Paar, U.; Langer, G.J. Ash dieback assessments on intensive monitoring plots in Germany: Influence of stand, site and time on disease progression. *J. Plant Dis. Prot.* **2024**, *131*, 1355–1372. [\[CrossRef\]](#)
33. Carroll, D.; Boa, E. Ash dieback: From Asia to Europe. *Plant Pathol.* **2024**, *73*, 741–759. [\[CrossRef\]](#)
34. Kjær, E.D.; McKinney, L.V.; Nielsen, L.R.; Hansen, L.N.; Hansen, J.K. Adaptive potential of ash (*Fraxinus excelsior*) populations against the novel emerging pathogen *Hymenoscyphus pseudoalbidus*. *Evol. Appl.* **2012**, *5*, 219–228. [\[CrossRef\]](#)
35. Ognjenović, M.; Seletković, I.; Potočić, N.; Marušić, M.; Tadić, M.P.; Jonard, M.; Rautio, P.; Timmermann, V.; Lovreškov, L.; Ugarković, D. Defoliation Change of European Beech (*Fagus sylvatica* L.) Depends on Previous Year Drought. *Plants* **2022**, *11*, 730. [\[CrossRef\]](#)
36. Zarnoch, S.J.; Bechtold, W.A.; Stolte, K. Using crown condition variables as indicators of forest health. *Can. J. For. Res.* **2004**, *34*, 1057–1070. [\[CrossRef\]](#)
37. Zhu, Z.; Klein, C.; Nölke, N. Assessing tree crown volume—A review. *For. Int. J. For. Res.* **2021**, *94*, 18–35. [\[CrossRef\]](#)
38. Zhang, Z.; Wang, T.; Skidmore, A.K.; Cao, F.; She, G.; Cao, L. An improved area-based approach for estimating plot-level tree DBH from airborne LiDAR data. *For. Ecosyst.* **2023**, *10*, 100089. [\[CrossRef\]](#)
39. Duan, Y.; Siegenthaler, A.; Skidmore, A.K.; Abdullah, H.; Chariton, A.A.; Laros, I.; Rousseau, M.; Arjen de Groot, G. Tree vitality predicts plant-pathogenic fungal communities in beech forest canopies. *For. Ecol. Manag.* **2025**, *585*, 122588. [\[CrossRef\]](#)
40. Timmermann, V.; Børja, I.; Hietala, A.M.; Kirisits, T.; Solheim, H. Ash dieback: Pathogen spread and diurnal patterns of ascospore dispersal, with special emphasis on Norway. *EPPO Bull.* **2011**, *41*, 14–20. [\[CrossRef\]](#)
41. Pfaffl, M.W. Quantification strategies in real-time PCR. *AZ Quant. PCR* **2004**, *1*, 89–113.
42. Barton, K. Package ‘mumin’. *Version* **2024**, *1*, 439.
43. Wickham, H. *ggplot2: Elegant Graphics for Data Analysis*; Springer: New York, NY, USA, 2016.
44. Havrdova, L.; Zahradnik, D.; Romportl, D.; Pešková, V.; Černý, K. Environmental and silvicultural characteristics influencing the extent of ash dieback in forest stands. *Balt. For.* **2017**, *23*, 168–182.
45. Lenz, H.D.; Bartha, B.; Straßer, L.; Lemme, H. Development of Ash Dieback in South-Eastern Germany and the Increasing Occurrence of Secondary Pathogens. *Forests* **2016**, *7*, 41. [\[CrossRef\]](#)
46. Klesse, S.; von Arx, G.; Gossner, M.; Hug, C.; Rigling, A.; Queloz, V. Amplifying feedback loop between growth and wood anatomical characteristics of *Fraxinus excelsior* explains size-related susceptibility to ash dieback. *Tree Physiol.* **2021**, *41*, 683–696. [\[CrossRef\]](#)
47. Grosdidier, M.; Ioos, R.; Husson, C.; Cael, O.; Scordia, T.; Marçais, B. Tracking the invasion: Dispersal of *Hymenoscyphus fraxineus* airborne inoculum at different scales. *Fems Microbiol. Ecol.* **2018**, *94*, fty049. [\[CrossRef\]](#)
48. Combes, M.J. The Ecology and Pathology of Ash Dieback Disease. Ph.D. Thesis, Cardiff University, Cardiff, UK, 2022.

49. Jochner-Oette, S.; Rohrer, T.; Eisen, A.-K.; Tönnies, S.; Stammel, B. Influence of Forest Stand Structure and Competing Understory Vegetation on Ash Regeneration—Potential Effects of Ash Dieback. *Forests* **2021**, *12*, 128. [[CrossRef](#)]
50. Kerr, G. The growth and form of ash (*Fraxinus excelsior*) in mixture with cherry (*Prunus avium*), oak (*Quercus petraea* and *Quercus robur*), and beech (*Fagus sylvatica*). *Can. J. For. Res.* **2004**, *34*, 2340–2350. [[CrossRef](#)]
51. Kim, J.H. Multicollinearity and misleading statistical results. *Korean J. Anesth.* **2019**, *72*, 558–569. [[CrossRef](#)]
52. Hemery, G.E.; Savill, P.S.; Pryor, S.N. Applications of the crown diameter–stem diameter relationship for different species of broadleaved trees. *For. Ecol. Manag.* **2005**, *215*, 285–294. [[CrossRef](#)]
53. McKinney, L.V.; Nielsen, L.R.; Collinge, D.B.; Thomsen, I.M.; Hansen, J.K.; Kjær, E.D. The ash dieback crisis: Genetic variation in resistance can prove a long-term solution. *Plant Pathol.* **2014**, *63*, 485–499. [[CrossRef](#)]
54. Avery, T.E.; Burkhardt, H.E. *Forest Measurements*, 5th ed.; McGraw-Hill Series in Forest Resources; McGraw-Hill: Boston, MA, USA, 2002.
55. Frank, E.F. Crown Volume Estimates. *Bull. Eastern Nat. Tree Soc.* **2010**, *9*, 3–8.
56. Kirisits, T.; Freinschlag, C. Ash dieback caused by *Hymenoscyphus pseudoalbidus* in a seed plantation of *Fraxinus excelsior* in Austria. *J. Agric. Ext. Rural Dev.* **2012**, *4*, 184–191. [[CrossRef](#)]
57. Fuller, R.; Henderson, A.C.B. Distribution of breeding songbirds in Bradfield Woods, Suffolk, in relation to vegetation and coppice management. *Bird Study* **1992**, *39*, 73–88. [[CrossRef](#)]
58. Susse, R.; Allegrini, C.; Morgan, P. *Management of Irregular Forests: Developing the Full Potential of the Forest*; Association Futaie Irregulière: Besançon, France, 2011.
59. Grosenbaugh, L.R. *Point Sampling and Line Sampling: Probability Theory, Geometric Implications, Synthesis*; Southern Forest Experiment Station, Forest Service, U.S. Department of Agriculture: New Orleans, LA, USA, 1958; Volume 160. Available online: https://www.srs.fs.usda.gov/pubs/misc/op_160.pdf (accessed on 19 April 2019).

Disclaimer/Publisher’s Note: The statements, opinions and data contained in all publications are solely those of the individual author(s) and contributor(s) and not of MDPI and/or the editor(s). MDPI and/or the editor(s) disclaim responsibility for any injury to people or property resulting from any ideas, methods, instructions or products referred to in the content.